Characterization of a Novel Analogue of 1α,25(OH)$_2$-Vitamin D$_3$ with Two Side Chains: Interaction with Its Nuclear Receptor and Cellular Actions

Anthony W. Norman,*[,†,§] Percy S. Manchand,[‖] Milan R. Uskokovic,[‖] William H. Okamura,[‡] Janet A. Takeuchi,[‡] June E. Bishop,[†] Jun-Iichi Hisatake,[⊥] H. Phillip Koeffler,[⊥] and Sara Peleg[#]

Departments of Biochemistry and Chemistry and Division of Biomedical Sciences, University of California, Riverside, California 92521, Hoffmann-La Roche Inc., Nutley, New Jersey 07110, Division of Hematology/Oncology, Cedars−Sinai Medical Center, UCLA School of Medicine, 8700 Beverly Boulevard, B-208, Los Angeles, California 90048, and Department of Medical Specialties, The University of Texas M. D. Anderson Cancer Center, Houston, Texas 77030

Received January 18, 2000

The hormone 1α,25(OH)$_2$-vitamin D$_3$ (125D) binds to its nuclear receptor (VDR) to stimulate gene transcription activity. Inversion of configuration at C-20 of the side chain to generate 20-epi-1α,25(OH)$_2$D$_3$ (20E-125D) increases transcription 200−5000-fold over 125D with its 20-normal (20N) side chain. This enhancement has been attributed to the VDR ligand-binding domain (LBD) having different contact sites for 20N and 20E side chains that generate different VDR conformations. We synthesized 1α,25-dihydroxy-21-(3-hydroxy-3-methylbutyl)vitamin D$_3$ (Gemini) with two six-carbon side chains (both 20N and 20E orientations). Energy minimization calculations indicate the Gemini side chain possesses significantly more energy minima than either 125D or 20E-125D (2346, 207, and 127 minima, respectively). We compared activities of 125D, 20E-125D, and Gemini, respectively, in several assays: binding to wild-type (100%, 147%, and 38%) and C-terminal-truncated mutant VDR; transcriptional activity (of the transfected osteopontin promoter in ROS 17/2.8 cells: ED$_{50}$ 10, 0.005, and 1.0 nM); mediation of conformational changes in VDR assessed by protease clipping (major trypsin-resistant fragment of 34, 34, and 28 kDa). For inhibition of cellular clonal growth of human leukemia (HL-60) and breast cancer (MCF7) cell lines, the ED$_{50}$(125D)/ED$_{50}$(Gem) was respectively 380 and 316. We conclude that while Gemini readily binds to the VDR and generates unique conformational changes, none of them is able to permit a superior gene transcription activity despite the presence of a 20E side chain.

Introduction

There are a wide range of biological effects which are mediated by the hormonally active form of vitamin D, namely 1α,25(OH)$_2$-vitamin D$_3$ (125D) through the vitamin D endocrine system. This endocrine system includes not only the classical arena of Ca^{2+} homeostasis (intestine, kidney, and bone) but also actions on the immune system, the pancreatic B cell and other endocrine cells, keratinocytes, the processes of cell differentiation of normal cells, and inhibition of proliferation of many types of neoplastic cells.[1] Central to the generation of these far-reaching biological effects is the interaction of 125D with its nuclear receptor (VDR), to produce a competent ligand−receptor complex that is able to selectively interact with a VDR response element present on the promoters of genes which are transcriptionally regulated by the steroid hormone.[2,3] The VDR is present in over 30 different cell types that participate in the vitamin D endocrine system.[4]

The two principal approaches to studying 125D regulation of gene transcription have been the following: (a) to employ libraries of analogues that display unique or selective properties in comparison to 125D[5−7] and (b) to dissect and define how 125D and analogues interact with the VDR to cause conformational changes in the receptor protein[6,7] that enhance VDR heterodimerization with the retinoid X receptor (RXR). In turn, this enhances heterodimer binding to other transcriptionally required proteins, such as co-activators,[8−10] and to DNA. These structure−function studies have shown that it is possible to design analogues of 125D that have both favorable biological responses in selected target organs and minimal calcemic side effects.[1]

An important focus of structure−function studies of synthetic ligands for the VDR is the stereocenter at carbon 20 of the side chain.[11,12] Analogues with a 20-epi (20E) [e.g. 20-epi-1α,25(OH)$_2$-vitamin D$_3$ (20E-125D)] rather than the 20-normal (20N) orientation (see Figure 1) have antiproliferative activities 200−5000-fold greater than 125D when assayed in a variety of cell types, including human leukemic HL-60 cells, rat osteoblastic ROS 17/2.8 cells, and human keratinocytes.[5,13,14] It was originally postulated that the potency of these analogues could be explained because: (i) their affinity for the VDR was significantly higher than that of 125D, (ii) their uptake into target cells was more efficient, or (iii) the catabolism rate of the 20E analogues was slower than that of 125D.[11,12] However, studies from our[15,16] and other[17,18] laboratories do not support these possible explanations.

* To whom correspondence should be addressed. Phone: (909) 787-4777. Fax: (909) 787-4784. E-mail: Norman@ucrac1.ucr.edu.
[†] Department of Biochemistry, University of California.
[‡] Department of Chemistry, University of California.
[§] Division of Biomedical Sciences, University of California.
[‖] Hoffmann-La Roche Inc.
[⊥] UCLA School of Medicine.
[#] The University of Texas M. D. Anderson Cancer Center.

10.1021/jm0000160 CCC: $19.00
Published on Web 06/21/2000

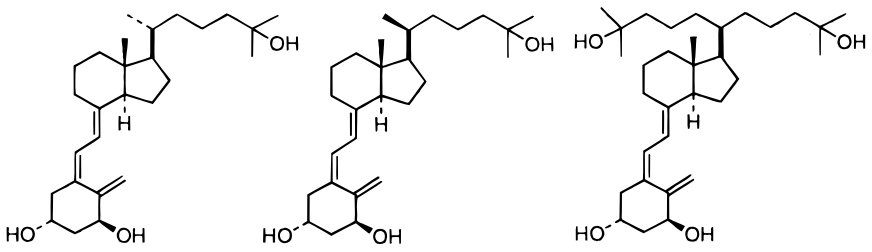

Figure 1. Structural formulas of 1α,25(OH)$_2$-vitamin D$_3$ (125D), 20-epi-1α,25(OH)$_2$-vitamin D$_3$ (20E-125D), and the two-side-chain analogue of 125D, 1α,25-dihydroxy-21-(3-hydroxy-3-methylbutyl)vitamin D$_3$ (Gemini).

Recent studies from our laboratories suggest that the primary basis by which 20E analogues achieve potency superior to 125D in stimulating gene transcription lies in their interaction with the VDR to generate unique conformational changes of the receptor protein that enhance its subsequent interactions with other transcription factors, particularly the RXR.[15,16] The principal evidence supporting this conclusion was the observation that three 20E analogues when bound in vitro to [^{35}S]-VDR resulted in trypsin sensitivity patterns different from those generated by the equivalent 20N analogues bound to the [^{35}S]VDR.[15] This was interpreted to be due to different receptor conformations being induced by the ligands. These same three 20E analogues, in comparison to their 20N analogues, also conferred upon the VDR an enhanced ability to form heterodimers with RXR, as assessed by electromobility shift assays, and to activate transcription via two different promoter constructs with vitamin D-response elements (VDRE), which were transfected into ROS 17/2.8 cells. Further support for the differential interaction of 20E versus 20N analogues with the VDR was obtained by preparation of several mutations of the C-terminal region of the VDR. This facilitated mapping of specific amino acids that interact with the ligand and resulted in the conclusion that the ligand-binding domain (LBD) of the VDR has multiple and different contact sites for the two families of side-chain-modified ligands.[16]

To further probe the role of the side chain of 125D in its interactions with the VDR, we have synthesized a unique analogue (Gemini) which has the same two six-carbon side chains at C-20, one with a 20N orientation and one with a 20E orientation (see Figure 1). Our objective was to determine the various properties of this two-side-chain analogue in interacting with the nuclear VDR both in vitro and in host cells containing the receptor. We report here that Gemini productively interacts with the VDR to generate a conformational shape different from that produced by either 125D or 20E-125D. Interestingly, despite this difference, the biological potency of the Gemini−VDR ligand−receptor complex is very similar to that of 125D in stimulating gene transcription.

Results

Figure 1 presents the structures of 125D, 20E-125D, and 1α,25(OH)$_2$-21-(3-hydroxy-3-methylbutyl)vitamin D$_3$ (Gemini) which are profiled in this report.

Figure 2 presents a summary of the overall synthetic route for the chemical synthesis of Gemini, a novel analogue of 125D with two six-carbon side chains. The protected olefin **3** is easily accessible in high yield from the Inhoffen−Lythgoe diol via **1** and then the iodide **2**. A double-ene reaction results in the conjugated diester **4.** This process is a stepwise process wherein a mono-ene intermediate (not shown) is rapidly formed at an early stage of the reaction. Compound **4** undergoes a smooth hydrogenation with palladium on carbon catalyst, and the saturated analogue **5** is converted cleanly to ditertiary alcohol **6**. The following steps via **8** and **10** in the synthesis of the final product Gemini (Figure 1) with the two side chains of 125D are reminiscent of the protocol used for the synthesis of 125D.[19] The structures of Gemini and the various intermediates shown in Figure 2 were fully confirmed by spectral and analytical analyses, including NMR and mass spectrometry.

The eight-carbon side chains of both 125D and 20E-125D are known to be highly conformationally flexible.[20] The side chains of the seco-steroids 125D and 20E-125D assume distinct orientations in their global or minimal energy conformation; the 20N side chain is oriented to the 'northeast' while the 20E side chain is oriented to the 'northwest'.[21−23] Figure 3 provides a conformational analysis using the previously described dot map formalism[21,24] of the individual side-chain arms of Gemini in comparison to the side chain of 125D (C/C′ vs A/A′) and 20E-125D (D/D′ vs B/B′). Within a 3-kcal/mol window, the double-side-chain analogue (C/C′ and D/D′) displays 2346 minima, whereas the parent 125D and 20E-125D exhibit only 207 and 127 conformers, respectively. These computations reveal the apparently greater flexibility of the individual side-chain arms of the double-side-chain analogue (compare the greater density of dots or conformers in C/C′ and D/D′ to those in A/A′ and B/B′, respectively).

The two hydroxyl groups of the double-side-chain analogue (C/C′ and D/D′ in Figure 3) occupy a very similar volume in space as their single 20N and 20E side-chain counterparts despite the differences in their global minimum orientations. The differences in their global minima are particularly evident upon inspection of the complementary side views (C′ vs A′ and D′ vs B′). Both hydroxyl groups of the side-chain arms of Gemini are localized above and below the plane of the CD ring. Like the side chain of the hormone 125D, the 20N side-chain portion of the double-side-chain analogue occupies a volume largely "east to northeast" of the CD ring; and like the side chain of the unnatural 20E-125D, the 20-epimer arm of the double-side-chain analogue resides in the "northwest" region. The two hydroxyl groups are localized in different, but not exclusively different, regions within 3 kcal/mol of the global minimum.

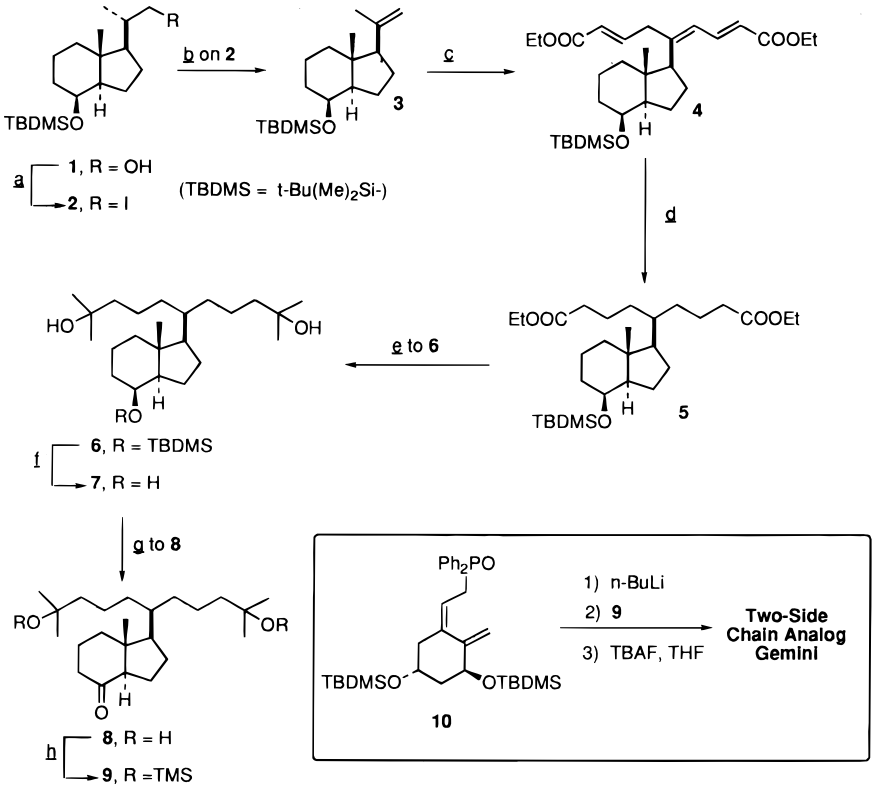

Figure 2. Summary of the chemical synthesis of Gemini. The synthetic scheme shows the transformation of alcohol **1** to protected ketone **9** followed by its Horner coupling to A-ring phosphine oxide **10**, which is then transformed to the two-side-chain analogue Gemini (structure shown in Figure 1). The chemical reagents, except where noted, are as follows: (a) Ph_3P, I_2 (94%); (b) KO^{t}Bu, DMSO (85%); (c) ethyl propiolate, $EtAlCl_2$ (32%); (d) H_2, Pd/carbon (94%); (e) MeMgBr (93%); (f) H_2SiF_6, MeCN (85%); (g) PDC (94%); (h) TMS-imidazole (92%).

Previous studies from these laboratories have established that 20E analogues are 50−3000-fold more potent than 125D in stimulating VDR-mediated gene transcription;[15,16] also the 20E analogues induce distinct conformational changes in the VDR as judged by trypsin protease sensitivity.[15] Figure 4 compares the potency of 125D, 20E-125D, and Gemini to transcriptionally activate the VDRE on the osteopontin promoter in a thymidine kinase promoter/growth hormone reporter construct. The fusion gene containing the VDRE was transfected into ROS 17/2.8 cells, and the growth hormone reporter-protein production was measured after treatment for 48 h with increasing concentrations of the three ligands. The relative order of potency for activating the osteocalcin promoter was 20E-125D > Gemini > 125D.

Figure 5 presents results of ligand-exchange rate studies in which recombinant hVDR transfected in COS-1 cells were treated with ligand (125D, 20E-125D, or Gemini) and then lysed. The cell lysates were incubated in vitro with [^{3}H]125D. It is apparent that there is both a difference in the exchange properties and stability of VDR occupied by 20E-125D as compared with either 125D or the two-side-chain analogue Gemini. Only 20% of the 20E-125D ligand was displaced by [^{3}H]-125D after a 60-min incubation, whereas approximately 55% of Gemini or 125D was displaced. Thus, the exchange properties of Gemini, which has both 20N and a 20E side chains, are similar to that of 125D, which has only the 20N side chain.

Previous studies have established that the VDR displays different trypsin-mediated fragmentation patterns when it is occupied with ligands with 20N or 20E side chains.[16,16] Figure 6 presents results of the protease sensitivity studies on ligand-occupied VDR. In vitro synthesized [^{35}S]VDR was exposed to increasing concentrations of either 125D, 20E-125D, or Gemini followed by treatment with trypsin and gel electrophesis (SDS−PAGE) (see Figure 6). The proteolytic fragment pattern resulting from trypsin treatment of the occupied VDR was different for the three seco-steroids. Occupancy of the VDR with 125D or 20E-125D resulted in a major fragment at 34 kDa, but in the presence of 20E-125D an additional fragment was seen at 32 kDa (see Figure 6, panel A); this result is in agreement with our previous report.[15] However, when the VDR was occupied with Gemini, a significant major fragment was seen at 28 kDa with no evidence for the 34-kDa fragment. Further, the concentration of ligand required to achieve 50% of the maximal concentration of the major proteolytic fragment (ED_{50}) was different for each seco-steroid (see Figure 6, panel B, and Table 1). The ED_{50} for 125D was 45-fold higher than that for 20E-125D, and the ED_{50} for Gemini was 30-fold higher than that for 125D and 1400-fold higher than that for 20E-125D. We conclude that analogue Gemini generates a unique conformational change in the VDR different from that achieved by either 125D or 20E-125D.

Figure 7 presents the consequences of two separate mutations of the wild-type (WT) VDR on the ligand-induced sensitivity of [^{35}S]VDR to protease clipping by trypsin under in vitro conditions. Our previous results indicated that truncation of the AF-2 domain (at the extreme carboxy terminus of the VDR) by introduction

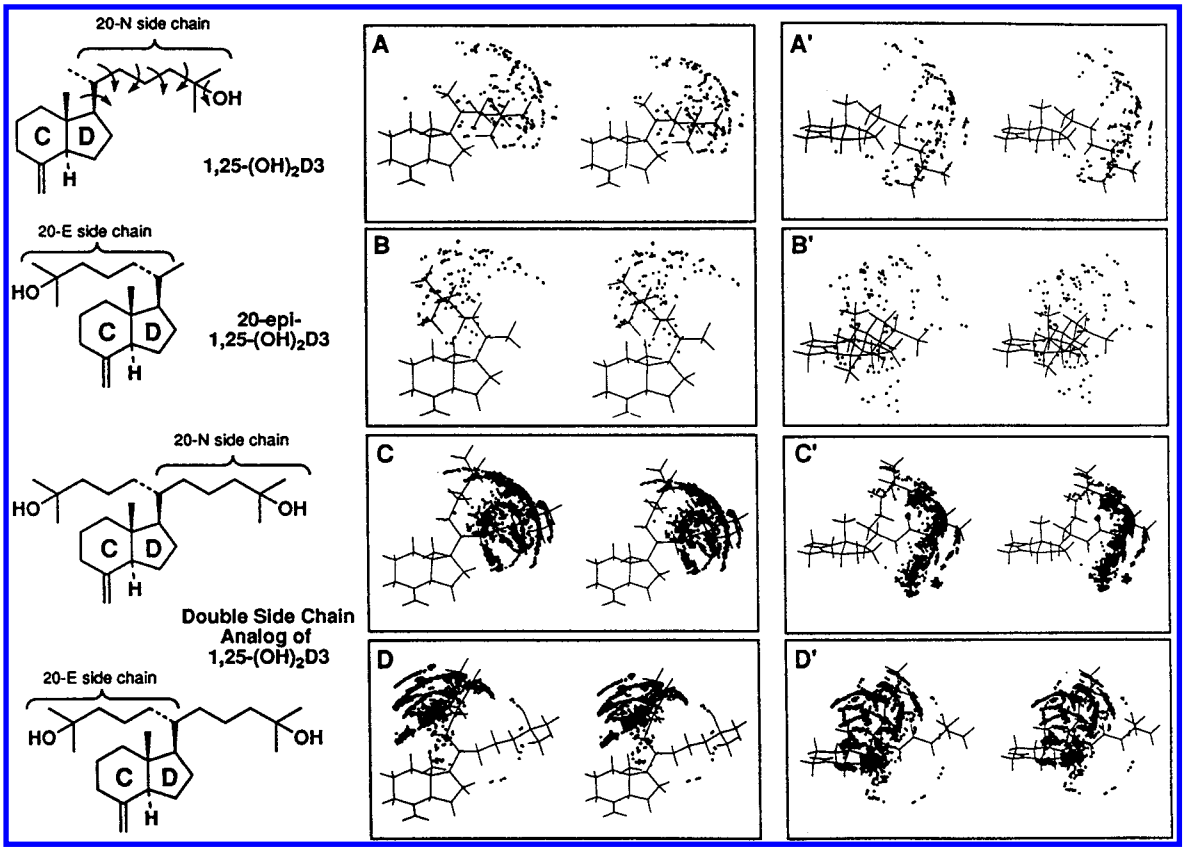

Figure 3. Stereoscopic dot maps of the side chains of 125D, 20E-125D, and the two-side-chain Gemini for a 3-kcal/mol window. Dot maps are used to depict the volume in space that the side chain can occupy. The dots locate possible occupation sites of the side-chain hydroxyl group, which is considered to be an important factor in binding of the ligand to various host proteins. Using the dot map representations, only a limited number of drawings are needed to display a large number of energy-minimized side-chain conformers. Dot maps were constructed as described in Materials and Methods. Panels A and A′ pertain to the CD side-chain fragment model system of 125D. B and B′ are a similar representation of the side chain of 20E-125D. Panels C, C′, D, and D′ portray separately the individual arms of the double-side-chain analogue Gemini. Panels C and C′ reflect only the 20N side-chain portion of Gemini, while panels D and D′ depict only the 20E side-chain portion of Gemini. Note that A−D are dot maps viewing the natural CD fragment from the top face, while A′−D′ are views from the bottom edge of the approximate plane defined by the CD ring.

of a stop codon at residue 390 or imposition of a double mutation (V421M/F422A) in the AF-2 domain resulted in a very significant loss of binding by the altered VDR for 125D but not 20E-125D.[16] Figure 7 presents a comparison of the pattern of the major proteolytic fragments which result from occupying, respectively, the WT VDR or the two mutants (V421M/F422A and 390/TGA) with 125D, 20E-125D, or Gemini. The major proteolytic fragments were 34, 32, and 28 kDa (WT VDR), 28, 32 + 28, and 28 kDa (V421M/F422A), and 26, 26, and 28 + 26 kDa (390/TGA), respectively, for 125D, 20E-125D, and Gemini. Thus, Gemini clearly produces a unique 28-kDa fragment in the WT VDR similar to that shown in Figure 6. This same 28-kDa fragment is also significantly imposed by Gemini, but not 125D, on the two mutants, indicating that it is likely the 20E side chain of Gemini is important for the stabilization of the 28-kDa fragment. For the V421M/F422A mutant VDR, the pattern of proteolytic fragments generated by occupancy of the VDR with 20E-125D and Gemini were also different, again indicating the unique response of this VDR construct to Gemini.

Figure 8 presents results of competition of 125D and its analogues 20E-125D and Gemini for binding to WT VDR and its AF-2 mutant (V421M/F422A). In comparison to the WT VDR, 125D binds poorly to the V421M/F422A mutant VDR, a result consistent with our earlier results.[16] Also, as noted earlier, 20E-125D can bind virtually equivalently to the WT VDR and the V421M/F422A mutant VDR. In a similar fashion, Gemini bound to the V421M/F422A mutant only marginally less than to the WT VDR. These results suggest that the 20E side chain of Gemini is able to achieve the same general affinity of binding as the 20E-125D, although as indicated in Figure 7 the proteolytic fragment pattern is markedly different from that achieved by 20E-125D (only 1 fragment at 28 kDa vs fragments at 34, 32, and 28 kDa).

Figure 9 presents a comparison of the dose-dependent efficacy of 125D and Gemini with respect to their inhibition of the growth of human leukemic (HL-60), breast (MCF7), and prostate (LNCaP) cancer cell lines. The clonal growth of both the HL-60 and MCF7 cell lines was inhibited via exposure to either 125D or Gemini; however, the ED_{50} for Gemini was approximately 300 times lower than that of 125D (see Table 1). The prostate cell line only presented a blunted inhibition of clonal growth response for both 125D and Gemini.

The relative affinities of the three seco-steroids for binding to the chick intestinal VDR and human vitamin D binding protein (DBP) were determined via standard

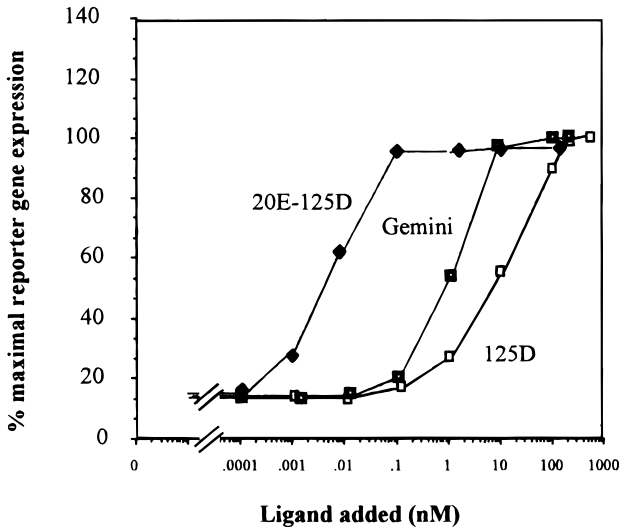

Figure 4. Transcriptional activity of 125D, 20E-125D, and the two-side-chain analogue Gemini. ROS 17/2.8 cells were transfected by the DEAE-dextran method with a thymidine kinase/growth hormone (*TK/GH*) fusion gene containing the osteopontin VDRE (opVDRE). The seco-steroids were present in the medium plus serum for 48 h prior to quantitation of the growth hormone by radioimmunoassay. Each point of the dose−response curve is the average of duplicate transfections. The results shown are representative of 3−5 transfection experiments. The ordinate values are normalized to the maximum growth hormone generated by 1α,25(OH)$_2$D$_3$ at 100 nM: □ = 125D; ● = 20E-125D; ■ = Gemini.

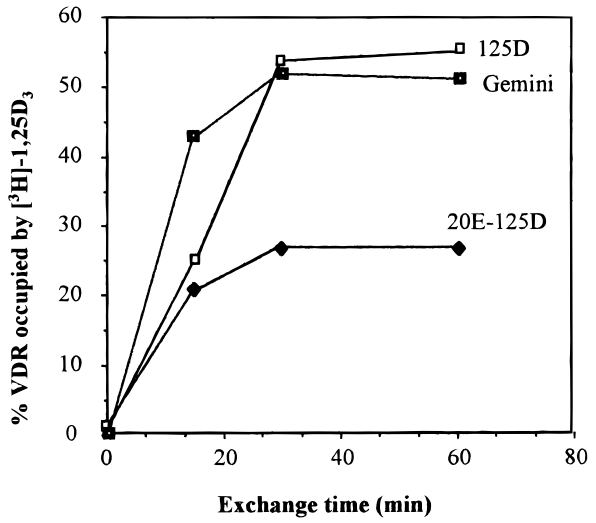

Figure 5. Exchange assay of 125D, 20E-125D, and the two-side-chain analogue Gemini with [^{3}H]125D. The exchange assay was conducted in COS-1 cells as described under Materials and Methods. Each ligand at 10^{-8} M was incubated with the cells for 1 h in a serum-free medium. Then the medium was removed, and the cells were washed, homogenized, and incubated with 0.2 pmol of [^{3}H]1,25(OH)$_2$D$_3$ with or without a 100-fold excess of nonradioactive 125D. Each point shown is the average of duplicate samples; the results shown are representative of four assays: □ = 125D; ● = 20E-125D; ■ = Gemini.

steroid competition assays (see Table 1). In these assays the *r*elative *c*ompetitive *i*ndex (RCI) is calculated.[25] By definition, the RCI of 125D is set to 100%. The main point of interest was to ascertain whether the two-side-chain Gemini could bind to the VDR or DBP. For Gemini, the VDR RCI was 38%, while the DBP RCI was only 2.5%. As reported previously, the VDR RCI for 20E-125D is 147% or 1.5-fold greater than the reference 125D.[1] However, for DBP the RCI for analogue 20E-125D was only 2.6%. Thus the LBD of the VDR is significantly more able than the LBD of DBP to accommodate either the 20E side chain or the two side chains.

Discussion

Over the past decade there have been many reports describing structure−function relationships between various structural functionalities of the molecule 125D and a variety of biological responses (see review covering 278 analogues and 820 structural modifications[26]). This information has been accumulated through synthesis and biological and biochemical testing of a wide variety of side-chain-modified analogues of 125D; these have included lengthening or shortening the eight-carbon side chain and introduction of double or triple bonds,[27] allene,[28] or aromatic ring[29] functionalities along the chain. While some of these analogues have displayed a favorable profile of selective biological responses, none have achieved the attention generated via inversion of the C-20 chiral center to produce a family of 20E analogues of 125D.[11] Some of these 20E analogues achieved separation of biological responses such that they have antiproliferative[12,18] or transcriptional activities[17,30] 200−5000-fold more potent than 125D but with a reduced calcemic activity.

It is noteworthy that the unusual potency of the 20E analogues is not directly explained by their affinity for the VDR. For example, 20E-125D and 20-epi-22-oxa-24a,26a,27a-trihomo-1α,25(OH)$_2$D$_3$ only bind to the VDR ≈ 147% or 120%, respectively, as well as 125D,[11] yet their antiproliferative activities are 200−5000-fold greater than that of 125D. The LBD of the 50-kDa VDR is a 37-kDa polypeptide encompassing two-thirds of the receptor molecule.[2] A three-dimensional molecular model of the VDR LBD has been prepared using the atomic coordinates of the thyroid receptor.[31] Our studies have shown that the C-terminal portion of the LBD, encoding the transcription AF-2 domain of the VDR, has multiple and different contact points for the 20N versus 20E family of analogues.[16] Thus, a 20E analogue when bound to the VDR generates a different overall conformation from that achieved by binding a 20N analogue. As a consequence, the 20E analogue complex with VDR is more stable, and the three-dimensional structure of the receptor with a 20E ligand is apparently more effective at forming heterodimers with RXR, interacting with other transcriptionally important proteins, such as co-activators,[9,32] and generating a transcriptionally active complex. The overall result is a significantly greater transcriptional potency through the osteopontin or osteocalcin VDRE.

To further study the relative importance of the 20N versus 20E side chain, we conceptualized synthesis of a 125D analogue that simultaneously possessed two side chains attached to C-20. We wished to learn whether the VDR LBD can accommodate an analogue with two side chains and whether the binding properties and the biological properties of Gemini are more 20E-like or 20N-like. Here we report the chemical synthesis and biological characterization of a novel analogue of 125D, which has two six-carbon side chains, one in the 20N

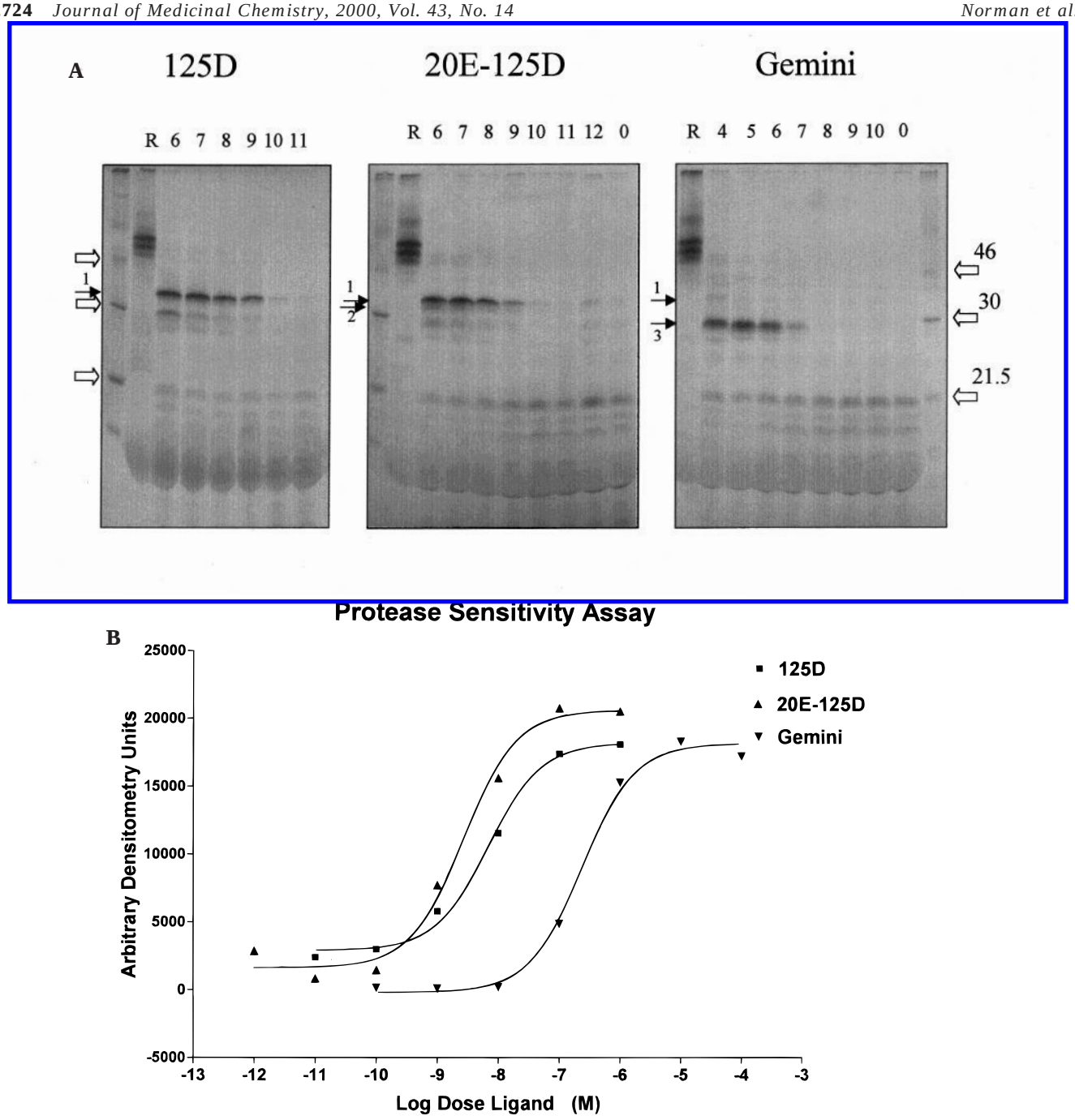

Figure 6. Ligand-induced sensitivity of the WT VDR to in vitro treatment with trypsin. (A) In vitro translated WT VDR labeled with [^{35}S]methionine was incubated without or with increasing concentrations of the seco-steroids 125D, 20E-125D, and Gemini before digestion with trypsin. The digestion products were analyzed by PAGE and autoradiography. The proteolytic products are indicated by arrows. The fragment sizes are 34, 32, and 28 kDa for fragments 1−3, respectively. The large arrows indicate molecular weight markers at 46, 30, and 21.5 kDa. Lanes marked R contained control [^{35}S]VDR. Analogue treatment concentrations are given above their respective lanes as −log M. (B) Each lane of the results shown in panel A was scanned with a densitometer, and the results are presented. The calculated ED_{50} values ± SD for 125D, 20E-125D, and Gemini were 5.9 ± 0.6, 0.13 ± 0.09, and 180 ± 50 nM, respectively, for fragments 34, 34, and 28 kDa.

orientation and the other in the 20E orientation. The side-chain analogue, 1α,25-dihydroxy-21-(3-hydroxy-3-methylbutyl)vitamin D_3 (designated as Gemini), was synthesized in seven steps from a known starting material; a preliminary report has appeared.[33] Independently, Calverley et al. also presented a brief report of the chemical synthesis of the same analogue.[34]

The side chains of both 125D and 20E-125D are known to be highly conformationally flexible and each assumes its minimal energy characteristic orientations, either to the 'northwest' for 20E or to the 'northeast' for 20N (see Figure 3).[20] The stereoscopic dot maps of the side chains of the two-side-chain Gemini provide insight into the significant differences in the properties of the single-side-chain analogues as compared with Gemini. While the individual side chains of Gemini assume the characteristic 'northwest' or 'northeast' orientation for their 20E or 20N chain, the two-side-chain Gemini is much more conformationally flexible as reflected by the 2346 minima, whereas the parent 125D and 20E-125D exhibit only 207 and 127 conformers, respectively. This increased flexibility of the two

Table 1. Summary of Biological Properties of 1α,25(OH)$_2$D$_3$, 1α,25(OH)$_2$-20-epi-D$_3$, and a Two-Side-Chain Analogue, Gemini[a]

		RCI (%)		ED$_{50}$ (nM)		colony formation, ED$_{50}$ (nM)		
seco-steroids	code	DBP	VDR	transcription activation	protease sensitivity	HL-60	MCF7	LNCaP
1α,25(OH)$_2$D$_3$	125D	100	100	10	5.9 ± 0.6	130	380	NR
20-epi-1α,25(OH)$_2$D$_3$	20E-125D	2.6 ± 1.5	147 ± 12	0.005	0.13 ± 0.09			
two-side-chain	Gemini	2.5 ± 1.4	38 ± 15	1	180 ± 50	0.34	1.2	82

[a] The human DBP RCI and the chick intestinal VDR RCI were determined from separate steroid competition assays as described under Materials and Methods. The transactivation assay is a measure of the ability of the indicated seco-steroid to activate the VDRE present in the promoter of the osteopontin gene coupled to growth hormone which was transfected into ROS 17/2.8 cells (Figure 4). The protease sensitivity assay reflects ligand-induced changes in the conformation of [^{35}S]VDR after treatment with trypsin followed by PAGE separation (Figure 6). The ED$_{50}$ for the protease sensitivity is tabulated for the concentration dependency of the major proteolytic fragment present (see Figure 6) which is 34, 34, and 28 kDa, respectively, for 125D, 20E-125D, and Gemini. The procedures for the inhibition of colony formation assays are described in Materials and Methods, and the dose−response results are in Figure 9. NR = ED$_{50}$ was not reached at ≤10^{-6} M compound.

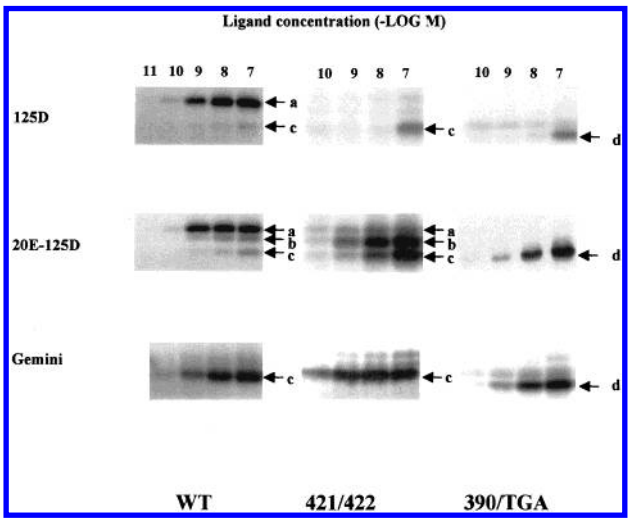

Figure 7. Effect of mutations in the WT VDR on ligand-induced sensitivity to in vitro treatment with trypsin. In vitro translated WT or mutated VDR was labeled with [^{35}S]methionine and incubated with the indicated concentrations of 125D or the analogues 20E-125D or Gemini (10^{-7}−10^{-11} M) before digestion with 20 μg/mL trypsin. The digestion products were analyzed by PAGE and autoradiography. The arrows indicate the position of the following ligand-dependent trypsin-resistant fragments: (a) 34, (b) 32, (c) 28, and (d) 26 kDa; WT, WT VDR; 421/422, AF-2-mutated VDR (V421M/F422A); 390/TGA, VDR containing a stop codon at position 390.

side chains may be useful when the Gemini is gaining initial access to the LBD of the VDR, since it effectively allows the molecule to be more malleable and possibly accommodate to the structural constraints imposed by the side chains of the amino acids facing the interior of the VDR LBD.

Two key components of the vitamin D endocrine system are the plasma vitamin D-binding protein (DBP), which transports all vitamin D metabolites throughout the circulatory system, and the nuclear VDR. We have compared for DBP and VDR the RCI, a measure of the relative ligand affinity for the binding proteins, for the two-side-chain Gemini with that of 20E-125D and 125D with respect to their binding to VDR or DBP (see Table 1). The presence of the second side chain on Gemini did not dramatically impair the ability of this analogue to bind to the VDR as the RCI was 38% of that of 125D, while the RCI for 20E-125D was 147%. Clearly a 20E side chain alone or in combination with a 20N side chain is competent to gain access to the LBD of the unoccupied VDR; the molecular VDR LBD model can readily accommodate Gemini as a ligand with an orientation of the A, seco B, and C/D rings identical to that of 125D.[35] This is all the more impressive when consideration is given to the additional molecular volume of Gemini (458 A^3) as compared with either 125D or 20E-125D (375 A^3) as determined via molecular modeling. It is known that some structural alterations of 125D that do not significantly increase the molecular volume can, however, result in a dramatic reduction in the VDR RCI; thus, the RCI for 1β,25(OH)$_2$D$_3$ is 0.08% and for 18-acetoxy-1α,25(OH)$_2$D$_3$ it is 0.04%.[1] Thus, the additional molecular volume associated with the presence of two side chains on Gemini is not a serious liability with respect to gaining access to the VDR LBD, suggesting that the volume of the VDR LBD may be larger than necessary to accommodate the natural hormone.

In contrast, for DBP, the RCI values of both the two-side-chain Gemini and the single-side-chain 20E-125D were dramatically reduced, with values of 2.5% and 2.6%, respectively. Clearly the presence of a 20E side chain is a severe liability for binding to the LBD of DBP. Thus the VDR and DBP binding proteins display significantly different ligand preferences for the three seco-steroids employed in this communication, which is consistent with the fact that there is no known structural similarity between these two proteins.

A further probing into the mode of interaction of 20E and 20N analogues with VDR has shown that the 20E analogues formed a significantly more stable complex with the VDR than the 20N analogues, including the natural hormone, 125D. This parameter of ligand−receptor interaction was examined in the present study by using an assay in which the rate of exchange of analogue-occupied receptor with the natural hormone is examined in vitro. Our experiments suggested that the stability of VDR occupied by Gemini resembles the stability of 125D-occupied VDR and not the 20E-occupied VDR. Our earlier studies suggested that the mechanism that supported the stability of VDR−20E complex was their binding away from the AF-2 domain. Therefore, we compared the binding requirements of the three compounds to WT VDR and VDR that had the AF-2 domain mutated (421/422) or deleted (390/TGA). To our surprise, Gemini bound to the AF-2-mutated VDR as well as it did to WT VDR. These results can be interpreted to suggest that there is no cause-and-effect relationship between the usage of the AF-2 domain for binding and VDR ligand stability. Alternatively, it is possible that Gemini uses the AF-2 residues in the intact receptor to form a complex with similar stability as the 125D−VDR complex, but once these residues are

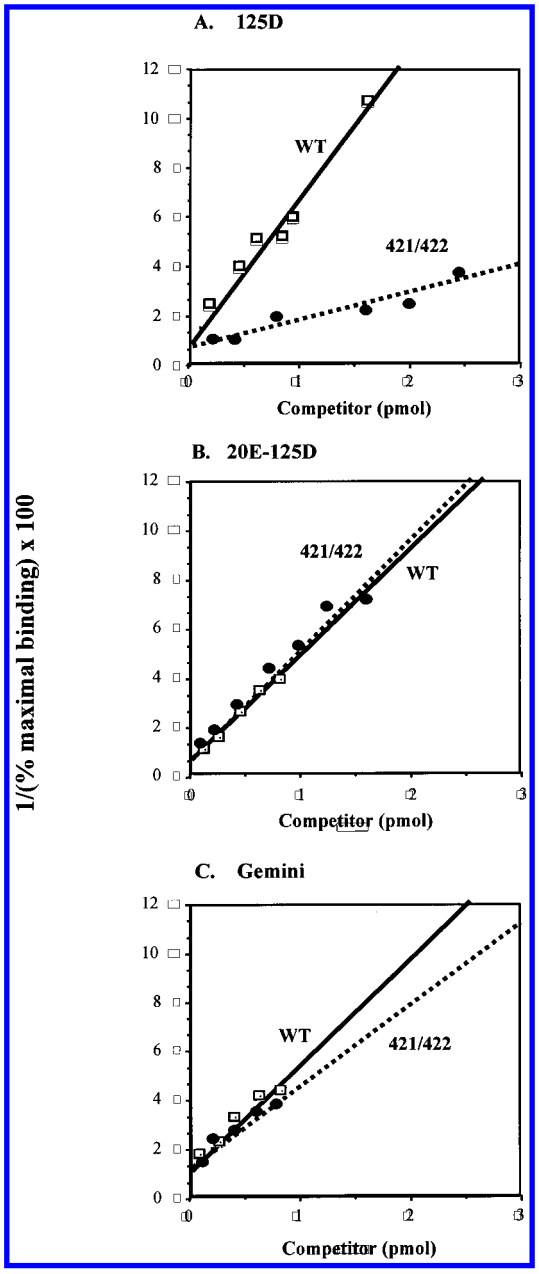

Figure 8. Competition of 125D and its analogues 20E-125D and Gemini for binding to WT hVDR and its AF-2 mutant (V421M/F422A). Competition assays were performed 3−4 times with each competitor 125D (A), 20E-125D (B), or Gemini (C) by incubating homogenates from COS-1 cells transfected with either WT VDR (WT) or the AF-2 mutant (V421M/F422A) with [^{3}H]125D and increasing amounts of the competitor indicated above each graph. Each competition assay of the mutant VDR was performed simultaneously with a competition assay of WT VDR. Linear regression coefficients (*r*) of the plots shown were 0.92−0.96.

removed, it changes to the contact points to those used by the 20E analogue.

A comparison of the ability of 125D, 20E-125D, and Gemini to effect conformational changes in the VDR was made by assessing the protease sensitivity of ligand occupied [^{35}S]VDR$_{nuc}$ to treatment with low concentrations of trypsin as studied by subsequent PAGE (see Figures 6 and 7). Our laboratories have previously reported dramatic differences in protease sensitivity of the ligand-occupied [^{35}S]VDR$_{nuc}$ for a series of 20N versus 20E analogues.[15,16] Thus, while the [^{35}S]VDR$_{nuc}$ occupied with either 20E-125D or 125D has the same major proteolytic fragment of 34 kDa, the 20E-125D induced the appearance of an additional fragment at 32 kDa. In contrast, as reported in this communication, the two-side-chain Gemini generates a major proteolytic fragment of 28 kDa for both the WT VDR and the two mutant VDRs (V421M/F422A and 390/TGA), suggesting that it generates a conformational shape of the ligand-occupied VDR which is different from those shapes generated either by the 20N or 20E seco-steroids. We speculate that because of the presence of two side chains, Gemini may have a more difficult time than a ligand with one side chain in gaining full entrance to the LBD.

The conformational differences induced by the three compounds should be quantitative or qualitative differences in their transcriptional potencies or efficacies. To test this possibility, we examined the transcriptional ED$_{50}$ potency for activation of the thymidine kinase promoter/growth hormone reporter construct containing the opVDRE (see Figure 4 and Table 1) by 125D, Gemini, and 20E-125D: 10, 1, and 0.005 nM, respectively. Gemini was 10-fold more potent than 125D, but 20E-125D was 200- and 2000-fold more potent than Gemini and 125D. Thus, the transcriptional potency of the two-side-chain Gemini is modestly enhanced by the presence of its 20E side chain present as compared to 125D. But, also the presence of the 20N side chain in Gemini results in a 200-fold reduction in the transcriptional activity achieved by 20E-125D. Although the Gemini-occupied VDR does achieve a conformational shape different from that of the 20E-125D-occupied or 125D-occupied VDR (28-kDa vs 34-kDa proteolytic fragment), it is apparent that the shape of this Gemini-occupied VDR is not one which is remarkably more potent in transactivation of the osteopontin promoter. Similar results were also noted for the osteocalcin promoter (data not presented). In conclusion, each receptor shape induced a different transcription profile. Additional studies will reveal whether these differences in transcription are due to different recruitment of dimerization partners or of transcriptional co-activators.

The biological effectiveness of both Gemini and 125D to inhibit the clonal growth of the HL-60, MCF7, and LNCaP cells (Figure 9) is consistent with the observation that these cell lines possess the VDR.[1,36−38] The ED$_{50}$(125D)/ED$_{50}$(Gem) for HL-60 and MCF7 cells was respectively 100 and 50. Thus for both cell lines, Gemini was significantly more potent than 125D. Their relative activities paralleled their relative gene transcriptional activities rather than their binding affinity for the VDR (see Table 1) which is consistent with the conclusions derived from the protease sensitivity that binding of Gemini by the VDR results in a different conformation that is more productive with respect to both activation of gene transcription and inhibition of clonal growth. In contrast, in the LNCaP prostate cell lines (Figure 9) neither Gemini nor 125D effected a full dose−response inhibition of clonal growth. The reason for the refractoriness of this cell line is unclear.

The presence of the second side chain on 125D introduces several issues which may bear on determining the overall in vivo biological properties of analogue Gemini. 125D is known to be inactivated principally by

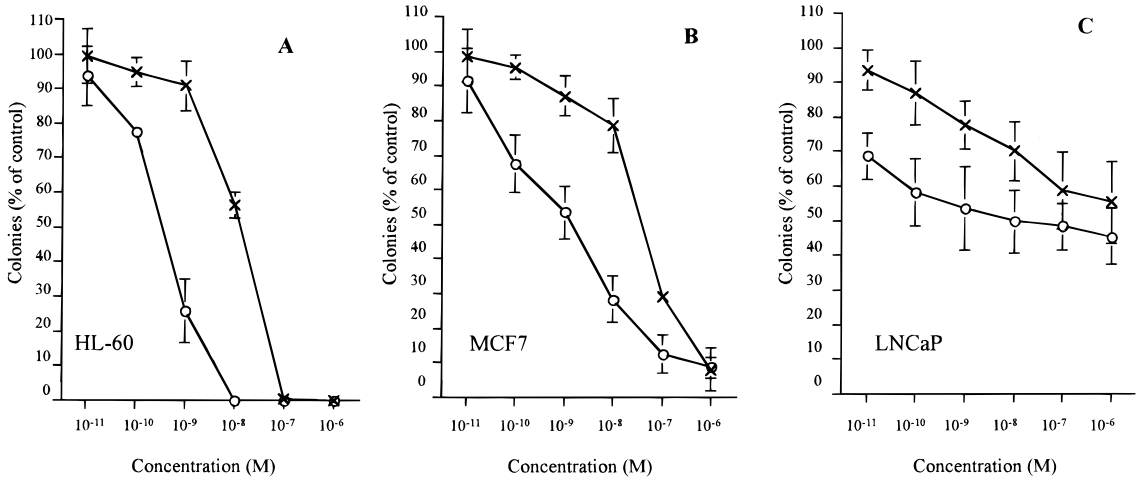

Figure 9. Dose−response of 1α,25(OH)$_2$D$_3$ and Gemini on clonal proliferation of (A) HL-60 human leukemic cells, (B) MCF7 breast cancer cells, and (C) LNCaP prostate cells. Results are expressed as percent of control plates containing no vitamin D compounds. Each point represents the mean ± SD of at least three independent experiments with triplicate dishes: 1α,25-(OH)$_2$D$_3$ (×−×) and Gemini (○−○).

several metabolic pathways which hydroxylate the side chain initiating side-chain cleavage.[39] Thus the presence of a second side chain may interfere with the orderly metabolism process resulting in a longer metabolic half-life and differences in potency between acute and chronic dosing due to accumulation of higher circulating levels of Gemini.

Our future studies with Gemini will further explore a detailed determination of the kinetic 'on' and 'off' rates for the ligand from the VDR and as well study the metabolism and circulating concentrations of this two-side-chain analogue in vivo. Also it is known that 125D, in addition to generating biological responses via VDR-mediated regulation of genomic events, can also produce rapid, nongenomic responses[40,41] though interaction with a putative membrane receptor.[42] Thus, it will also be pertinent to determine the efficacy of the two-side-chain Gemini to mediate rapid biological responses.

Materials and Methods

Reagents. [^{35}H]Methionine and [23,24(*n*)-^{3}H]1,25(OH)$_2$D$_3$ were obtained from Amersham Corp. A coupled transcription/translation kit and a site-directed mutagenesis kit were obtained from Promega. The two-side-chain analogue of 125D was synthesized by Hoffmann-La Roche, Nutley, NJ. The structural formulas for the key seco-steroids studied in this communication are shown in Figure 1.

Chemical Synthesis of Two-Side-Chain Analogue of 125D. The synthetic scheme employed for the chemical synthesis of 1α,25-dihydroxy-21-(3-hydroxy-3-methylbutyl)vitamin D$_3$ (designated as Gemini) is summarized in Figure 2.

Iodide 2. To an ice-cold solution of 60 g (0.23 mmol) of triphenylphosphine and 41 g (0.60 mol) of imidazole in 400 mL of CH_2Cl_2 was added 58 g (0.46 mol) of iodine. The cooled mixture, which became heterogeneous after 5 min, was stirred for 35 min and treated with a solution of 33 g (0.10 mol) of alcohol **1** in 125 mL of CH_2Cl_2 during 15 min and then the mixture was stirred at room temperature for 5 h. The mixture was quenched with 400 mL of 2.5% sodium thiosulfate and then worked up in the standard manner. The resulting vacuum-dried residue was chromatographed (silica gel, 5% ethyl acetate in hexanes) to afford a colorless oil, which crystallized in the cold to afford the purified iodide **2**: 41.3 g (94%); mp 43−44 °C; $[\alpha]^{25}_D$ +50.58 ($CHCl_3$, $c = 3.25$); ^{1}H NMR ($CDCl_3$) δ 0.00 (6 H, s), 0.89 (9 H, s), 0.95 (3 H, s), 0.99 (3 H, d, $J = 5.6$ Hz), 3.17 (1 H, dd, $J = 9.4$, 5.0 Hz), 3.32 (1 H, dd, $J = 9.4$, 2.0 Hz), 4. 0 (1 H, s); MS (FAB) *m*/*z* 435 (M, 50). Anal. Calcd for $C_{19}H_{37}IOSi$: C, 52.28; H, 8.54; I, 29.07; Si, 6.43. Found: C, 52.27; H, 8.72; I, 28.99; Si, 6.45.

[1*R*-(1α,3a*β*,4α,7aα)]-(1,1-Dimethylethyl)dimethyl[[octahydro-7a-methyl-1-(1-methylethenyl)-1*H*-inden-4-yl]oxy]silane (3). To a stirred solution of 40 g (92 mmol) of iodide **2** in 285 mL of dry THF and 125 mL of dry DMSO was added 20.5 g (183 mmol) of KO^{t}Bu. The mixture was stirred under argon for 1.25 h and then poured into a mixture of 500 mL of hexanes and 500 mL of water. Standard workup afforded 31 g of a pale yellow oil, which was chromatographed (silica gel, hexanes) to afford 23.9 g (85%) of **3** as a colorless oil: $[\alpha]^{25}_D$ +36.95 ($CHCl_3$, $c = 1.67$); IR ($CHCl_3$) 1639 cm^{-1}; ^{1}H NMR ($CDCl_3$) δ 0.00 (6 H, s), 0.79 (3 H, s), 0.88 (9 H, s), 1.15 (1 H, m), 1.40 (4 H, m), 1.60−1.70 (3 H, m), 1.73 (3 H, s), 1.74−1.90 (3 H, m), 1.97 (1 H, t, $J = 9$ Hz), 4.01 (1 H, s), 4.68 (1 H, s), 4.85 (1 H, s); MS *m*/*z* 308 (M, 10). Anal. Calcd for $C_{19}H_{36}OSi$: C, 73.95; H, 11.76; Si, 9.10. Found: C, 73.91; H, 11.90, Si, 9.16.

[1*R*-[1α(2*E*,4*E*,7*E*),3a*β*,4α,7aα]]-5-[4-[[(1,1-Dimethylethyl)dimethylsilyl]oxy]octahydro-7a-methyl-1*H*-inden-1-yl]-2,4,7-nonatrienedioic Acid Diethyl Ester (4). To a stirred solution of 3.08 g (10.0 mmol) of **3** and 3.92 g (40.0 mmol) of ethyl propiolate in 20 mL of CH_2Cl_2 was added 40.0 mL (40.0 mmol) of a 1.0 M solution of ethylaluminum dichloride in hexanes. The mixture was stirred under argon at room temperature for 24 h, treated with an additional 981 mg (10 mmol) of ethyl propiolate and 7.5 mL (7.5 mmol) of a 1.0 M solution of ethylaluminum dichloride in hexanes, and stirred for an additional 18 h. The resultant orange-red solution was added cautiously to a mixture of 200 mL of ethyl acetate and 100 mL of 50% brine, and after the fizzing had subsided, the organic phase was collected and then worked up in the standard fashion to give 5.76 g of a red gum. Fractional chromatography (silica gel, 10% EtOAc in hexanes) afforded 2.2 g of crude **4**, which upon HPLC purification (YMC silica gel, 50-cm × 50-mm column) with 7.5% ethyl acetate in hexanes afforded 1.62 g (32%) of **4** as a pale yellow gum: $[\alpha]^{25}_D$ +83.50 ($c = 0.98$, EtOH); UV (MeOH) 284 ($\epsilon = 28200$) nm; IR ($CHCl_3$) 1708, 1651, 1628 cm^{-1}; ^{1}H NMR ($CDCl_3$) δ 0.006 (6 H, s), 0.80 (3 H, s), 0.88 (9 H, s), 1.16 (1 H, t, $J = 7.6$ Hz), 1.28 (6 H, overlapping t, $J = 7$ Hz), 2.16 (1 H, t, $J = 9$ Hz), 3.00, (1 H, dd, $J = 6$, 16 Hz), 3. 35 (1 H, dd, $J = 16$, 4 Hz), 4. 02 (1 H, s), 4.16 (4 H, overlapping q, $J = 7$ Hz), 5.75 (1 H, d, $J = 16$ Hz), 5.84 (1 H, d, $J = 15$ Hz), 6.17(1 H, d, $J = 11$ Hz), 6.88 (1 H, dt, $J = 16$, 6 Hz), 7.50 (1 H, dd, $J = 15$, 11 Hz); MS (EI) *m*/*z* 504 (M, 23). Anal. Calcd for $C_{29}H_{48}O_5Si$: C, 69.00; H, 9.58; Si, 5.56. Found: C, 68.94; H, 9.69; Si, 5.67.

[1*R*-(1α,3a*β*,4α,7aα)]-5-[4-[[(1,1-Dimethylethyl)dimethylsilyl]oxy]octahydro-7a-methyl-1*H*-inden-1-yl]-nonanedioic Acid Diethyl Ester (5). A stirred solution of 1.01 g (2.0 mmol) of triene ester **4** in 50 mL of ethyl acetate

was hydrogenated over 200 mg of 10% palladium on charcoal at room temperature and ambient pressure until hydrogen absorption ceased (140 mL during 2.5 h). The mixture was filtered with ethyl acetate washings, which upon concentration gave 1.07 g of a colorless oil. This was purified by flash chromatography (silica gel, 12% ethyl acetate in hexanes) to give 964 mg (94%) of **5** as a colorless oil: $[\alpha]^{25}_D$ +32.1 ($CHCl_3$, c = 1.04); IR ($CHCl_3$) 1726 cm^{-1}; ^1H NMR ($CDCl_3$) δ 0.00 (3 H, s), 0.01 (3 H, s), 0.87 (9 H, s), 0.88 (3 H, s), 1.27 (6 H, t, J = 7 Hz), 2.25 (4 H, br t), 3.98 (1 H, s), 4.11 (4 H, q, J = 7 Hz); MS (FAB) m/z 511 (M + 1, 100). Anal. Calcd for $C_{29}H_{54}O_5Si$: C, 68.11; H, 10.66; Si, 5.50. Found: C, 68.21; H, 10.85; Si, 5.43.

[1*R*-(1α,3a*β*,4α,7aα)]-6-[4-[[(1,1-Dimethylethyl)dimethylsilyl]oxy]octahydro-7a-methyl-1*H*-inden-1-yl]-2,10-dimethyl-2,10-undecanediol (6). To a stirred ice-cooled solution of 868 mg (1.7 mmol) of diester **5** in 12 mL of anhydrous THF was added dropwise 5.0 mL (15 mmol) of a 3.0 M solution of methylmagnesium bromide in diethyl ether. The mixture was stirred at room temperature for 45 min, cooled to 5 °C, and quenched by the dropwise addition of 3 mL of saturated NH_4Cl. After the fizzing had subsided, 15 mL of ethyl acetate and 15 mL of saturated NH_4Cl were added. Stirring was continued for 20 min, and then the mixture was poured into 100 mL of ethyl acetate and 50 mL of saturated NH_4Cl. Standard workup afforded 814 mg of a colorless gum, which was purified by flash chromatography (silica gel, 50% ethyl acetate in hexanes). High vacuum-drying (17 h) of the resulting residue consisted of 763 mg (93%) of **6** as a colorless foam: $[\alpha]^{25}_D$ +35.8 (EtOH, c = 1.02); IR ($CHCl_3$) 3608 cm^{-1};^1H NMR ($CDCl_3$) δ 0.00 (6 H, s), 0.88 (9 H, s), 0.90 (3 H, s), 1.20 (12 H, s), 3.99 (1 H, s); MS (EI) m/z 482 (3, M). Anal. Calcd for $C_{29}H_{58}O_3Si$: C, 72.14; H, 12.11; Si, 5.82. Found: C, 72.18; H, 11.99; Si, 5.69.

[1*S*-(1α,3a*β*,4α,7aα)]-Octahydro-1-[5-hydroxy-1-(4-hydroxy-4-methylpentyl)-5-methylhexyl]-7a-methyl-4*H*-inden-4-ol (7). To a stirred solution of 700 mg (1.45 mmol) of **6** in 5 mL of THF and 15 mL of CH_3CN contained in a Teflon bottle was added 3.0 mL of a 30% aqueous solution of fluorosilicilic acid and the mixture was stirred under argon at room temperature for 1 h. Four 2.0-mL portions of the fluorosilicilic acid solution were then added at hourly intervals, for a total of 11 mL of reagent and a reaction time of 5 h. The reaction mixture was diluted with 15 mL of water and poured into a mixture of 60 mL of water and 125 mL of ethyl acetate. After the fizzing had subsided, the organic phase was collected and the aqueous phase was re-extracted with 3 × 75 mL of ethyl acetate. Standard workup afforded 534 mg of a gum, which was purified by flash chromatography (silica gel, 70% ethyl acetate in hexanes) to give 458 mg (85%) of **7** as a colorless foam: $[\alpha]^{25}_D$ +26.2 ($CHCl_3$, c = 0.76); IR ($CHCl_3$) 3608 cm^{-1}; ^1H NMR ($CDCl_3$) δ 0.93 (3 H, s), 1.21 (12 H, s), 1.79−1.95 (4 H, m); MS (FAB) m/z 369 (M + H).

[1*S*-(1α,3a*β*,7aα)]-Octahydro-1-[5-hydroxy-1-(4-hydroxy-4-methylpentyl)-5-methylhexyl]-7a-methyl-4*H*-inden-4-one (8). To a stirred solution of 400 mg (1.08 mmol) of **7** in 8.0 mL of CH_2Cl_2 was added 1.30 g (3.45 mmol) of pyridinium dichromate and the mixture was stirred at room temperature for 4.75 h. It was diluted with 20 mL of diisopropyl ether, stirred for a further 15 min and filtered over a pad of Celite. The Celite was washed with 4 × 40 mL of diisopropyl ether and the combined filtrate and washings were evaporated to give 405 mg of a pale yellow gum, which was purified by flash chromatography (silica gel, 75% ethyl acetate in hexanes) to give 372 mg (94% yield) of **8**: $[\alpha]^{25}_D$ +0.45 (EtOH, c = 0.92); IR ($CHCl_3$) 3608, 1706 cm^{-1}; ^1H NMR ($CDCl_3$) δ 0.63 (3 H, s), 1.22 (12 H, s), 2.20−2.28 (2 H, m), 2.45 (1 H, dd, J = 7.6,11 Hz); MS (EI) m/z 348.3 (M − H_2O, 3). Anal. Calcd for $C_{23}H_{42}O_3$: C, 75.36; H, 11.55. Found: C, 75.13; H, 11.47.

[1*S*-(1α,3a*β*,7aα)]-Octahydro-7a-methyl-1-[5-methyl-1-[4-methyl-4-[(trimethylsilyl)oxy]pentyl]-5-[(trimethylsilyl)oxy]hexyl]-4*H*-inden-4-one (9). To a stirred solution of 367 mg (1.0 mmol) of ketone **8** in 10 mL of CH_2Cl_2 was added 1.25 mL (8.5 mmol) of 1-(trimethylsilyl)imidazole and the mixture was stirred under argon at room temperature for 4 h. It was diluted with 7 mL of water, stirred for a further 15 min, and poured into a mixture of 75 mL of ethyl acetate and 50 mL of 50% brine. The organic phase was collected and the aqueous phase was re-extracted with 3 × 50 mL of ethyl acetate. The combined organic extracts after standard workup gave a colorless oil, which was chromatographed (silica gel, 20% ethyl acetate in hexanes) to give 469 mg (92%) of **9** as a colorless oil: $[\alpha]^{25}_D$ −3.21 ($CHCl_3$, c = 0.87); IR ($CHCl_3$); 1706 cm^{-1}; ^1H NMR ($CDCl_3$) δ 0.01 (18 H, s), 0.63 (3 H, s), 1.20 (6 H, s), 1.21 (6 H, s), 2.21−2.31 (2 H, m), 2.46 (1 H, dd, J = 12, 11 Hz); MS (EI) m/z 495 (M − l5). Anal. Calcd for $C_{29}H_{58}O_3Si$: C, 68.17; H, 11.44; Si, 10.99. Found: C, 68.19; H, 11.41; Si, 11.07.

(1α,3*β*,5*Z*,7*E*)-21-(3-Hydroxy-3-methylbutyl)-9,10-secocholesta-5,7,10(19)-triene-1,3,25-triol (Double-Side-Chain Analogue, Gemini). To a stirred, dry-ice-cooled solution of 466 mg (0.80 mmol) of the Horner reagent[19] **10** in 4.0 mL of anhydrous THF was added 0.5 mL (0.80 mmol) of a 1.6 M solution of butyllithium in hexanes. The resultant deep red solution was stirred at −78 °C for 7 min, treated with 204 mg (0.40 mmol) of ketone **9** in 3.0 mL of anhydrous THF, and stirred at −78 °C for 3 h. The mixture was allowed to warm to room temperature, quenched with 5 mL of a 1:1 mixture of 2 N Rochelle salt solution and 2 N $KHCO_3$ solution, stirred for an additional 15 min, and poured into a mixture of 80 mL of ethyl acetate and 50 mL of a 1:1 mixture of 2 N Rochelle salt solution and 2 N $KHCO_3$ solution. The organic phase was collected and the aqueous phase was re-extracted with 3 × 60 mL of ethyl acetate. Standard workup afforded a gum, which was purified by flash chromatography (silica gel, 8% ethyl acetate in hexanes) to give 208 mg of a colorless gum. The latter was dissolved in 4.0 mL of THF and treated with 4.0 mL of a 1.0 M solution of TBAF in THF, and the solution was stirred under argon for 17 h. It was diluted with 5 mL of water, stirred for an additional 15 min, and poured into a mixture of 80 mL of 80% ethyl acetate in hexanes and 50 mL of water. Standard workup gave 139 mg of a semisolid, which was purified by flash chromatography (silica gel, 6% 2-propanol in ethyl acetate) to give 108 mg of a colorless foam. This was subjected to HPLC purification (silica gel, 50-cm × 50-mm column, 3% 2-propanol in ethyl acetate) to give after vacuum-drying 82 mg of Gemini as a colorless, amorphous solid: $[\alpha]^{25}_D$ +13.8 (EtOH, c = 0.5); UV (MeOH) 263 (ϵ = 17500) nm; IR ($CHCl_3$) 3608 cm^{-1}; ^1H NMR ($CDCl_3$) δ 0.53 (3 H, s), 1.21 (12 H, s), 2.30 (1 H, dd, J = 10, 7 Hz), 2.59 (1 H, d, J = 11 Hz), 2.83 (1 H, d, J = 13 Hz), 5.00 (1 H, s), 5.33 (1 H, s), 6.02 (1 H, d, J = 11 Hz), 6.37 (1 H, d, J = 11 Hz); HRMS (El): calcd for $C_{32}H_{54}O_2$ m/z 502.4022; found m/z 502.4024.

Energy Minimization Calculations for 125D and Analogue Side Chains. Stereoscopic dot maps of the side chains of 125D, 20E-125D, and Gemini were prepared by previously described procedures.[24,21] In brief, the dot maps are constructed by overlaying all accessible low-energy conformations for the side chain of the analogue under study by using a Monte Carlo conformational search routine using the MM2 force field in the BAKMDL and PC model programs (Serena Software, Bloomington, IN). The resulting dot maps are used to depict the volume in space that the side chain can occupy.

Determination of Transcriptional Activity. Rat osteosarcoma ROS 17/2.8 cells were plated in 35-mm dishes at a density of 3 × 10^5 cells/dish. The cells were transfected with 2 μg of plasmid containing the VDRE from the human osteopontin gene (opVDRE).[43] This response element was attached to the thymidine kinase promoter/growth hormone fusion gene. All transfections were performed by the DEAE-dextran method as previously described.[15] Immediately after transfection, the ligands (125D, 20E-125D or Gemini) (10^{-7}−10^{-13} M) were added to serum-free medium for 1 h and then removed. The cells were washed twice with phosphate-buffered saline (PBS), and DMEM with 10% fetal bovine serum was added. Forty-eight hours after transfection, culture medium was collected and the growth hormone levels were determined with a radioimmunoassay. Maximal fold induction of tran-

scription varied between experiments (3−5-fold), but maximal transcriptional activity was the same for 125D (which was included in each transfection experiment) and the analogues in individual experiments.

Site-Directed Mutations in the VDR. The WT VDR, the residue 421/422,AF-2-mutated VDR (V421M/F422A), and the C-terminal-truncated VDR 390/TGA were prepared as described previously.[16]

Ligand-Altered Protease Sensitivity Assay. Synthetic WT and mutant VDR labeled with [^{35}S]methionine (1000 Ci/mmol) was prepared by in vitro coupled transcription/translation in reticulocyte lysates (Promega) with the human VDR cDNA inserted into the pGEM-4 plasmid. The translated receptor preparations were incubated with the indicated concentrations of 125D or analogues for 20 min at room temperature. Then 15 μg/mL trypsin (Calbiochem) was added, and the mixtures were incubated for another 20 min. The digestion products were analyzed by 14% sodium dodecyl sulfate−polyacrylamide gel electrophoresis (SDS−PAGE), and the gels were dried and autoradiographed.

Ligand Binding Assays. To assess the relative affinity of 125D and the two analogues under study (20E-125D and Gemini) for the chick intestinal VDR, human DBP, and the WT or mutant VDR, a determination of the *r*elative *c*ompetitive *i*ndex (RCI) was carried out according to our standard procedures.[44] Both of these procedures are steroid competition assays where increasing concentrations of the analogue or standard nonradioactive 125D are incubated for 4 h at 4 °C with a defined concentration of [^{3}H]125D and the binding protein. Then separation of bound and free ligand is achieved by use of either hydroxyapatite (VDR) or charcoal-dextran (DBP) and the RCI calculated.[25] By definition the RCI of 125D is set to 100%.

Exchange Assays for Nonradioactive Ligands Bound to the VDR with [^{3}H]125D. VDR-transfected COS-1 cells were separately incubated with 10^{-8} M 125D, 20E-125D, or Gemini in a serum-free medium for 1 h. Then the medium was removed, and the cells were washed three times in ice-cold PBS and homogenized. The number of unoccupied binding sites was determined by incubating duplicate samples of cell homogenate for the time indicated at 30 °C with 0.2 pmol of [^{3}H]125D with or without a 100-fold excess of nonradioactive 125D and then incubated for 3 h on ice. The free ligand was separated from bound by hydroxyapatite, and the amount of bound ligand was quantified by liquid scintillation spectrometry. Each point is the average of two samples.

Colony Formation Assay in Soft Agar. Cells were cultured in six-well culture dishes in a two-layer soft agar system as described previously.[45,46] The under layer contained 0.5% agar, the upper layer 0.3% agar (Difco Laboratories, Detroit, MI). Compounds and cells to be tested were mixed into the under layers and upper layers, respectively. Cell concentrations were 1×10^3/plate for HL-60, MCF7 and LNCaP cells. Cultures were placed in a humidified atmosphere, 5% CO_2, at 37 °C for 12 days. All experiments were carried out using triplicate plates per experimental point, and each experiment was performed at least three times. Colony formation (>40 cells) were scored with an inverted microscope.

Acknowledgment. This study was supported by NIH Grants DK09012-34 (A.W.N.) and DK-16595, UC Intramural Research Fund and Solvay Pharmaceutical Co. (W.H.O.), and Grant DK-50583 (S.P.).

Supporting Information Available: Details of spectroscopic methods, chromatographic profile, and additional NMR data for the two-side-chain analogue Gemino. This material is available, free of charge, via the Internet at http://pubs.acs.org.

References

(1) Bouillon, R.; Okamura, W. H.; Norman, A. W. Structure−Function Relationships in the Vitamin D Endocrine System. *Endocr. Rev.* **1995**, *16*, 200−257.

(2) Haussler, M. R.; Whitfield, G. K.; Haussler, C. A.; Hsieh, J. C.; Thompson, P. D.; Selznick, S. H.; Dominguez, C. E.; Jurutka, P. W. The Nuclear Vitamin D Receptor: Biological and Molecular Regulatory Properties Revealed. *J. Bone Miner. Res.* **1998**, *13*, 325−349.

(3) Freedman, L. P.; Lemon, B. D. Structural and Functional Determinants of DNA Binding and Dimerization by the Vitamin D Receptor. In *Vitamin D*; Feldman, D., Glorieux, F. H., Pike, J. W., Eds.; Academic Press: San Diego, 1997; pp 127−148.

(4) Reichel, H.; Koeffler, H. P.; Norman, A. W. The Role of the Vitamin D Endocrine System in Health and Disease. *N. Engl. J. Med.* **1989**, *320*, 980−991.

(5) Elstner, E.; Lee, Y. Y.; Hashiya, M.; Pakkala, S.; Binderup, L.; Norman, A. W.; Okamura, W. H.; Koeffler, H. P. 1α,25-Dihydroxy-20-Epi-Vitamin D_3: An Extraordinarily Potent Inhibitor of Leukemic Cell Growth in Vitro. *Blood* **1994**, *84*, 1960−1967.

(6) Peleg, S.; Liu, Y. Y.; Reddy, S.; Horst, R. L.; White, M. C.; Posner, G. H. A 20-Epi Side Chain Restores Growth-Regulatory and Transcriptional Activities of an A Ring-Modified Hybrid Analogue of 1α,25-Dihydroxyvitamin D_3 Without Increasing Its Affinity to the Vitamin D Receptor. *J. Cell. Biochem.* **1996**, *63*, 149−161.

(7) Munker, R.; Kobayashi, T.; Elstner, E.; Norman, A. W.; Uskokovic, M.; Zhang, W.; Andreeff, M.; Koeffler, H. P. A New Series of Vitamin D Analogues Is Highly Active for Clonal Inhibition, Differentiation, and Induction of WAF1 in Myeloid Leukemia. *Blood* **1996**, *88*, 2201−2209.

(8) Zhao, X. Y.; Eccleshall, T. R.; Krishnan, A. V.; Gross, C.; Feldman, D. Analysis of Vitamin D Analog-Induced Heterodimerization of Vitamin D Receptor With Retinoid X Receptor Using the Yeast Two-Hybrid System. *Mol. Endocrinol.* **1997**, *11*, 366−378.

(9) Baudino, T. A.; Kraichely, D. M.; Jefcoat, S. C., Jr.; Winchester, S. K.; Partridge, N. C.; MacDonald, P. N. Isolation and Characterization of a Novel Coactivator Protein, NCoA-62, Involved in Vitamin D-Mediated Transcription. *J. Biol. Chem.* **1998**, *273*, 16434−16441.

(10) Lemon, B. D.; Fondell, J. D.; Freedman, L. P. Retinoid X Receptor-Vitamin D_3 Receptor Heterodimers Promote Stable Preinitiation Complex Formation and Direct 1,25-Dihydroxyvitamin D_3-Dependent Cell-Free Transcription. *Mol. Cell. Biol.* **1997**, *17*, 1923−1937.

(11) Binderup, L.; Latini, S.; Binderup, E.; Bretting, C.; Calverley, M.; Hansen, K. 20-Epi-Vitamin D_3 Analogues: a Novel Class of Potent Regulators of Cell Growth and Immune Responses. *Biochem. Pharmacol.* **1991**, *42*, 1569−1575.

(12) Binderup, L. Vitamin D Analogues: New Regulators of Cancer Cell Growth and Differentiation. *Bioorg. Med. Chem. Lett.* **1993**, *3*, 1891−1896.

(13) Elstner, E.; Linker-Israeli, M.; Le, J.; Umiel, T.; Michl, P.; Said, J. W.; Binderup, L.; Reed, J. C.; Koeffler, H. P. Synergistic Decrease of Clonal Proliferation, Induction of Differentiation, and Apoptosis of Acute Promyelocytic Leukemia Cells After Combined Treatment With Novel 20-Epi Vitamin D_3 Analogues and 9-Cis Retinoic Acid. *J. Clin. Invest.* **1997**, *99*, 349−360.

(14) Elstner, E.; Linker-Israeli, M.; Said, J.; Umiel, T.; De Vos, S.; Shintaku, P.; Heber, D.; Binderup, L.; Uskokovic, M. R.; Koeffler, H. P. 20-Epi-Vitamin D_3 Analogues: A Novel Class of Potent Inhibitors of Proliferation and Inducers of Differentiation of Human Breast Cancer Cell Lines. *Cancer Res.* **1995**, *55*, 2822−2830.

(15) Peleg, S.; Sastry, M.; Collins, E. D.; Bishop, J. E.; Norman, A. W. Distinct Conformational Changes Induced by 20-Epi Analogues of 1α,25-Dihydroxyvitamin D_3 Are Associated With Enhanced Activation of the Vitamin D Receptor. *J. Biol. Chem.* **1995**, *270*, 10551−10558.

(16) Liu, Y. Y.; Collins, E. D.; Norman, A. W.; Peleg, S. Differential Interaction of 1α,25-Dihydroxyvitamin D_3 Analogues and Their 20-*Epi* Homologues With the Vitamin D Receptor. *J. Biol. Chem.* **1997**, *272*, 3336−3345.

(17) Ryhänen, S.; Mahonen, A.; Jääskeläinen, T.; Mäenpää, P. H. Synthetic 20-Epi Analogues of Calcitriol Are Potent Inducers of Target-Gene Activation in Osteoblastic Cells. *Eur. J. Biochem.* **1996**, *238*, 97−103.

(18) Elstner, E.; Heber, D.; Koeffler, H. P. 20-Epi-Vitamin D_3 Analogues: Potent Modulators of Proliferation and Differentiation of Breast Cancer Cell Lines in Vitro. *Adv. Exp. Med. Biol.* **1996**, *399*, 53−70.

(19) Baggiolini, E. G.; Iacobelli, J. A.; Hennessy, B. M.; Batcho, A. D.; Sereno, J. F.; Uskokovic, M. R. Stereocontrolled Total Synthesis of 1α,25-Dihydroxycholecalciferol and 1α,25-Dihydroxyergocalciferol. *J. Org. Chem.* **1986**, *51*, 3098−3108.

(20) Okamura, W. H.; Midland, M. M.; Hammond, M. W.; Rahman, N. A.; Dormanen, M. C.; Nemere, I.; Norman, A. W. Chemistry and Conformation of Vitamin D Molecules. *J. Steroid Biochem. Mol. Biol.* **1995**, *53*, 603−613.

(21) Midland, M. M.; Plumet, J.; Okamura, W. H. Effect of C20 Stereochemistry on the Conformational Profile of the Side Chains of Vitamin D Analogues. *Bioorg. Med. Chem. Lett.* **1993**, *3*, 1799−1804.
(22) Yamamoto, K.; Sun, W. Y.; Ohta, M.; Hamada, K.; DeLuca, H. F.; Yamada, S. Conformationally Restricted Analogues of 1α,-25-Dihydroxyvitamin D_3 and Its 20-Epimer: Compounds for Study of the Three-Dimensional Structure of Vitamin D Responsible for Binding to the Receptor. *J. Med. Chem.* **1996**, *39*, 2727−2737.
(23) Yamada, S.; Yamamoto, K.; Masuno, H.; Ohta, M. Conformation-Function Relationship of Vitamin D: Conformational Analysis Predicts Potential Side-Chain Structure. *J. Med. Chem.* **1998**, *41*, 1467−1475.
(24) Okamura, W. H.; Palenzuela, J. A.; Plumet, J.; Midland, M. M. Vitamin D: Structure−Function Analyses and the Design of Analogues. *J. Cell. Biochem.* **1992**, *49*, 10−18.
(25) Wecksler, W. R.; Norman, A. W. Structural Aspects of the Binding of 1α,25-Dihydroxyvitamin D_3 to its Receptor System in Chick Intestine. In *Methods in Enzymology: Vitamins and Co-Enzymes*; Academic Press: New York, 1980; pp 494−500.
(26) Spirichev, V. B.; Sergeev, I. N. Vitamin D: Experimental Research and Its Practical Application. *Wld. Rev. Nutr. Diet* **1988**, 173−216.
(27) Zhou, J. Y.; Norman, A. W.; Chen, D.; Sun, G.; Uskokovic, M. R.; Koeffler, H. P. 1α,25-Dihydroxy-16-Ene-23-Yne-Vitamin D_3 Prolongs Survival Time of Leukemic Mice. *Proc. Natl. Acad. Sci. U.S.A.* **1990**, *87*, 3929−3932.
(28) Craig, A. S.; Norman, A. W.; Okamura, W. H. The Synthesis of Two Novel Allenic Side Chain Analogues of 1α,25-Dihydroxyvitamin D_3. *J. Org. Chem.* **1992**, *57*, 4374−4380.
(29) Figadère, B.; Norman, A. W.; Henry, H. L.; Koeffler, H. P.; Zhou, J. Y.; Okamura, W. H. Arocalciferols: Synthesis and Biological Evaluation of Aromatic Side-Chain Analogues of 1α,25-Dihydroxyvitamin D_3. *J. Med. Chem.* **1991**, *34*, 2452−2463.
(30) Peleg, S.; Liu, Y.-Y.; Reddy, S.; Collins, E. D.; Norman, A. W. Differential Interaction of 1α,25-Dihydroxyvitamin D_3 and its 20-Epi-Analogue with the Transcription Activation Function 2(AF-2) Domain of the Vitamin D Receptor. In *Vitamin D: Chemistry, Biology and Clinical Applications of the Steroid Hormone*; Norman, A. W., Bouillon, R., Thomasset, M., Eds.; University of California: Riverside, 1997; pp 203−209.
(31) Wagner, R. L.; Apriletti, J. W.; McGrath, M. E.; West, B. L.; Baxter, J. D.; Fletterick, R. J. A Structural Role for Hormone in the Thyroid Hormone Receptor. *Nature* **1995,** *378*, 690−697.
(32) Gill, R. K.; Atkins, L. M.; Hollis, B. W.; Bell, N. H. Mapping the Domains of the Interaction of the Vitamin D Receptor and Steroid Receptor Coactivator-1. *Mol. Endocrinol.* **1998**, *12*, 57−65.
(33) Uskokovic, M. R.; Manchand, P. S.; Peleg, S.; Norman, A. W. Synthesis and preliminary evaluation of the biological properties of a 1α,25-dihydroxyvitamin D_3 analogue with two side-chains. In *Vitamin D: Chemistry, Biology and Clinical Applications of the Steroid Hormone*; Norman, A. W., Bouillon, R., Thomasset, M., Eds.; University of California: Riverside, 1997; pp 19−21.
(34) Kurek-Tyrlik, A.; Makaev, F. Z.; Wicha, J.; Zhabinskii, V.; Calverley, M. J. Pivoting 2-Normal and 20-Epi Calcitriols: Synthesis and Crystal Structure of a "Double Side Chain" Analogue. In *Vitamin D: Chemistry, Biology and Clinical Applications of the Steroid Hormone*; Norman, A. W., Bouillon, R., Thomasset, M., Eds.; University of California: Riverside, 1997; pp 30−31.
(35) Norman, A. W.; Adams, D.; Collins, E. D.; Okamura, W. H.; Fletterick, R. J. Three-Dimensional Model of the Ligand Binding Domain of the Nuclear Receptor for 1α,25-Dihydroxy-Vitamin D_3. *J. Cell Biochem.* **1999**, *74*, 323−333.
(36) Taoka, T.; Collins, E. D.; Irino, S.; Norman, A. W. 1,25$(OH)_2$-Vitamin D_3 Mediated Changes in mRNA for c-*Myc* and 1,25-$(OH)_2D_3$ Receptor in HL-60 Cells and Related Subclones. *Mol. Cell. Endocrinol.* **1993**, *95*, 51−57.
(37) Nolan, E.; Donepudi, M.; Vanweelden, K.; Flanagan, L.; Welsh, J. Dissociation of Vitamin D_3 and Anti-Estrogen Mediated Growth Regulation in MCF-7 Breast Cancer Cells. *Mol. Cell. Biochem.* **1998**, *188*, 13−20.
(38) Miller, G. J.; Stapleton, G. E.; Ferrara, J. A.; Lucia, M. S.; Pfister, S.; Hedlund, T. E.; Upadhya, P. The Human Prostatic Carcinoma Cell Line LNCaP Expresses Biologically Active, Specific Receptors for 1α,25-Dihydroxyvitamin D_3. *Cancer Res.* **1992**, *52*, 515−520.
(39) Henry, H. L.; Norman, A. W. Metabolism of vitamin D. In *Disorders of Bone and Mineral Metabolism*; Coe, F. L., Favus, M. J., Eds.; Raven Press: New York, 1991; pp 149−162.
(40) Zanello, L. P.; Norman, A. W. Stimulation by 1α,25$(OH)_2$-Vitamin D_3 of Whole Cell Chloride Currents in Osteoblastic ROS 17/2.8 Cells: A Structure−Function Study. *J. Biol. Chem.* **1997**, *272*, 22617−22622.
(41) Norman, A. W. Rapid Biological Responses Mediated by 1α,25-$(OH)_2$-Vitamin D_3: A Case Study of Transcaltachia (the Rapid Hormonal Stimulation of Intestinal Calcium Transport). In *Vitamin D*; Feldman, D., Glorieux, F. H., Pike, J. W., Eds.; Academic Press: San Diego, 1997; pp 233−256.
(42) Nemere, I.; Dormanen, M. C.; Hammond, M. W.; Okamura, W. H.; Norman, A. W. Identification of a Specific Binding Protein for 1α,25-Dihydroxyvitamin D_3 in Basal-Lateral Membranes of Chick Intestinal Epithelium and Relationship to Transcaltachia. *J. Biol. Chem.* **1994**, *269*, 23750−23756.
(43) Ozono, K.; Liao, J.; Kerner, S. A.; Scott, R. A.; Pike, J. W. The Vitamin D-Responsive Element in the Human Osteocalcin Gene. Association With a Nuclear Proto-Oncogene Enhancer. *J. Biol. Chem.* **1990**, *265*, 21881−21888.
(44) Norman, A. W.; Okamura, W. H.; Hammond, M. W.; Bishop, J. E.; Dormanen, M. C.; Bouillon, R.; Van Baelen, H.; Ridal, A. L.; Daane, E.; Khoury, R.; Farach-Carson, M. C. Comparison of 6-s-*Cis* and 6-s-*Trans* Locked Analogues of 1α,25$(OH)_2$-Vitamin D_3 Indicates That the 6-s-*Cis* Conformation Is Preferred for Rapid Nongenomic Biological Responses and That Neither 6-s-Cis nor 6-s-*Trans* Locked Analogues Are Preferred for Genomic Biological Responses. *Mol. Endocrinol.* **1997**, *11*, 1518−1531.
(45) Munker, R.; Norman, A. W.; Koeffler, H. P. Vitamin D Compounds: Effect on Clonal Proliferation and Differentiation of Human Myeloid Cells. *J. Clin. Invest.* **1986**, *64*, 424−430.
(46) Kubota, T.; Koshizuka, K.; Koike, M.; Uskokovic, M. R.; Miyoshi, I.; Koeffler, H. P. 19-Nor-26,27-Bishomo-Vitamin D_3 Analogues: A Unique Class of Potent Inhibitors of Proliferation of Prostate, Breast, and Hematopoietic Cancer Cells. *Cancer Res.* **1998**, *58*, 3370−3375.

JM0000160